

## **Synthesis and Characterization of Structural, Electrical and Magnetic Properties of NiO Nanocrystallites**

Muhammad Javid, Shahid Atiq<sup>1),\*</sup> and Shahzad Naseem

*Centre of Excellence in Solid State Physics, University of the Punjab,  
Lahore-54590, Pakistan*

<sup>1)</sup>E-mail: [shahidatiqpasrur@yahoo.com](mailto:shahidatiqpasrur@yahoo.com)

### **ABSTRACT**

Many materials exhibit unique properties when reduced to nano-scale, mainly due to increased surface to volume ratio. These unique properties enable nano-materials to be more beneficial from application view point. Nickel oxide has emerged as a classic example of a class of nano-materials whose structural, electrical and magnetic properties are of great interest. In the present study, we mainly focus on the preparation of nickel oxide nano-crystallites by a novel low cost sol-gel auto-combustion technique. Owing to the importance of fuel reagents in this material's synthesis method, various molar concentrations of citric acid have been employed to achieve the phase pure samples. X-ray diffraction revealed that prepared sample consisted of nickel oxide without any impurity. Scherrer's formula confirmed that the nickel oxide samples consisted of crystallites in the nano-meter range. Dielectric and magnetic properties were investigated using LCR meter and vibrating sample magnetometer, respectively.

### **1. INTRODUCTION**

Rapid development in the field of nanotechnology greatly depends upon the leading edge of nano-materials (Murray 2000). Quite often, exciting properties are emerged when particle size is reduced to nanometer scale, corresponding to their bulk counterparts. Metal oxide nanocrystalline materials exhibit fascinating properties and have established their importance as gas-sensors (Poulston *et al.* 2005), solar cells (Bandara and Yasomanee 2007), fuel cells (Levy 1997) and electrodes (Liao 2006). NiO nanostructures bear a wide range of applications having a p-type semiconducting properties and with a stable wide band gap of 3.6 to 4.0 eV. It has also been used as a transparent p-type semiconductor layer (Meybodi 2012). In addition, NiO shows anodic electrochromism and finds its applications in smart windows, dye-sensitized photocathodes and electrochemical super-capacitors (Qiao 2009). These functional properties depend mainly upon the surface morphology, matrix-pore interface and the porosity.

Nanocrystalline powers of NiO have been synthesized by various techniques such as chemical precipitation (Bahadur 2008), microwave assisted techniques (Mohammadyani 2009), anodic arc plasma method (Qiao 2009) and sonochemical methods (Aslani 2010). Sol-gel auto-combustion has recently emerged as a promising route to prepare oxide nanocrystalline powders in a phase pure form. Therefore, in the present study, we have employed this novel technique for the preparation of NiO nanocrystallites, in order to explore their electric and magnetic properties.

## 2. EXPERIMENTAL PROCEDURES

NiO nanocrystalline powders were prepared by sol-gel auto-combustion method. The use of fuel agent in this process plays a key role in the establishment phase pure crystallinity of the materials. In this study, we have emphasized on the molar concentration of the fuel agent in order to get pure well-crystalline NiO samples. All the chemicals, which include nickel nitrate [Ni(NO<sub>3</sub>).6H<sub>2</sub>O] and citric acid [C<sub>6</sub>H<sub>8</sub>O<sub>7</sub>], were of analytical grade purity and purchased from BDH [United Kingdom]. The molar concentration ratio of citric acid was varied from 1 to 2.5 moles as compared to 1 mole of nickel nitrate to prepare four samples, named as Sp-1, Sp-2, Sp-3 and Sp-4, as shown in first two columns of Table 1. The stoichiometric molar ratios of the reagents were separately dissolved in 50 ml of de-ionized water. The aqueous solutions were then mixed with vigorous stirring for about 30 min. The pH of the aqueous solutions was continuously monitored and maintained at 4 by adding an appropriate amount of liquid ammonia [NH<sub>3</sub>]. The xerogel of the solution was attained by constant stirring and evaporation at 90 °C on a hot plate. When the xerogel was obtained, the temperature was increased to 250 °C, which resulted in the self-combustion of the xerogel, ultimately converting into fine and fluffy powder. The black powder of NiO was then sintered in a Muffle furnace for 3 hours at 600 °C. Afterwards, the sintered products were put into modern mortar to grind it uniformly to produce a fine powder of having uniform grain sizes. The synthesized powders were characterized using, Rigaku D/Max-II A, X-ray diffractometer (XRD) for structural analysis. The diffractometer was operated at 40 kV and 40 mA using Cu K<sub>α1</sub> radiation having  $\lambda=1.540598 \text{ \AA}$  with a step scan size of 0.02°. Dielectric properties were determined by using 1920 LCR meter to check storage ability of materials. A 7404-Lakeshore vibrating sample magnetometer (VSM) was used to obtain the hysteresis loops for the magnetic studies of samples.

## 3. RESULTS AND DISCUSSION

The diffraction patterns of all the prepared samples have been shown in Fig. 1. The patterns were obtained at 2 $\theta$  values between 5° and 80°, with a step scan size of 0.05. The patterns indicate that the product contains single phase NiO, as the four sharp peaks, at 2 $\theta$  = 37.358°, 43.391°, 63.024°, 75.525°, belong to NiO, as sited in ICSD Reference Code No. 01-075-0269. The sharp peaks and strong intensity shows the excellent crystallinity of the powder samples. The diffraction peaks are corresponding to (111), (200), (220) and (311) planes. The indexing of the XRD data is based on fcc type structure with the space group Fm3m and space group no. 225. The unit cell parameter for NiO was evaluated as  $a = 4.1707, 4.1666, 4.1653$  and  $4.1708 \text{ \AA}$ , using the software "CELL". The values are quite in agreement as has been reported earlier (Ulman 2011, Peck 2011).

The crystallite size has been estimated from the X-ray peak broadening, considering the most intense diffraction peak (200) for all the samples, using the Scherrer formula (Pei 2008). The evaluated values of the crystallite sizes of all the four samples were found almost same, having values of  $11.90 \pm 0.01 \text{ nm}$ , as shown in Table 1. These values of crystallite sizes are comparable as determined by other research groups (Tiwari 2006, Richardson 2003). A very small variation in the crystallite size was observed in the samples. The reason for the small values of the

Table 1 Crystallite size as a function of moles of citric acid

Sample No.	No. of moles of citric acid	Bragg's angle ( $\theta$ )	Full width half maximum 'B' (degrees)	Full width half maximum 'B' (radians)	Crystallite size $= \frac{0.94\lambda}{B \cos \theta}$ (nm)
Sp-1	1	21.696	0.750	0.0131	11.90 nm
Sp-2	1.5	21.722	0.750	0.0131	11.91 nm
Sp-3	2	21.7265	0.750	0.0131	11.90 nm
Sp-4	2.5	21.6875	0.750	0.0131	11.91 nm

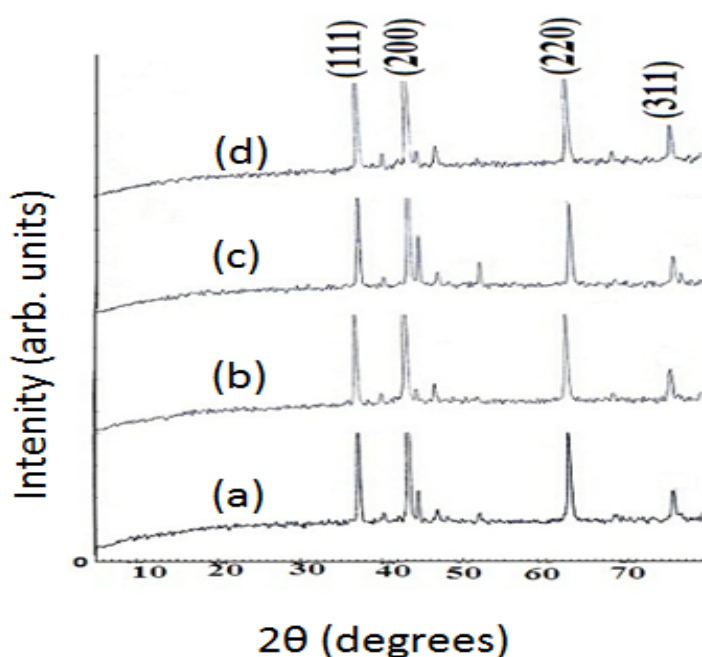


Fig. 1 XRD Patterns of (a) Sample Sp-1, (b) Sp-2, (c) Sp-3 and Sp-4

crystallite sizes can be understood considering the relatively larger values of the full width at half maximum (FWHM). Fig. 2 shows the variation of crystallite size as a function of molar concentration of the citric acid, used as a fuel. It might be inferred from the results that the molar concentration of the citric acid as a fuel does not affect the crystallite size of the NiO nanocrystallites.

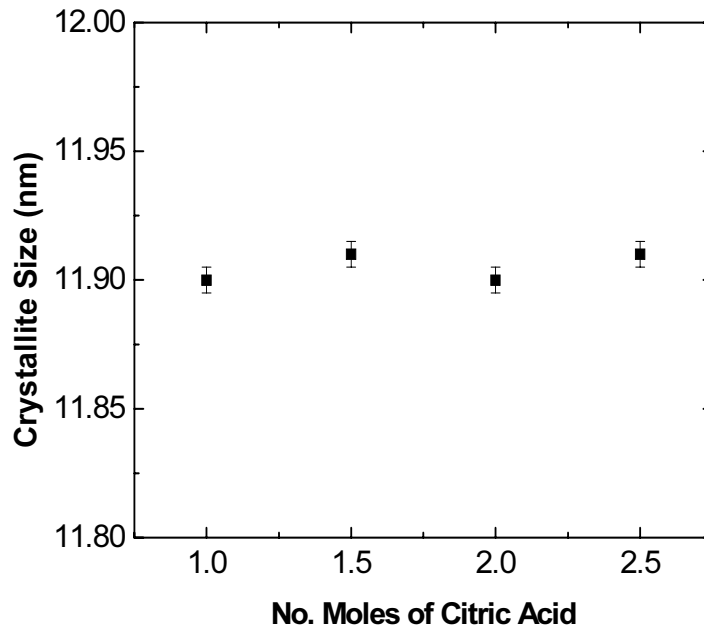


Fig. 2 Effect of concentration of citric acid on the crystallite size

The variation of dielectric constant ( $\epsilon'$ ) as a function of frequency is provided in Fig. 3, for all the samples. The value of  $\epsilon'$  is higher at lower frequencies and is found to decrease with increase in frequency. At high frequencies, the value becomes small, constant and independent of frequency (Laishram 1999). The variation in dielectric constant is directly related with space charge polarization. The presence of higher conductivity phases (grains) in the insulating matrix (grain boundaries) of a dielectric produces localized accumulation of charge under the influence of an electric field that results in space charge polarization. These space charge carriers usually need a finite time to line up their axes in the direction of the applied electric field. If the field is continuously increased, a point is reached, where space charge carriers cannot remain preserved with the field. Afterwards, the alternation of their direction lags behind the field, which results in the reduction of dielectric constant of the material (Shaikh 1999).

Fig. 4 illustrates the dielectric loss ( $\epsilon''$ ) factors of all the four samples. The dielectric loss factor is an important part of the core losses in dielectric materials. As obvious in the Figures, the dielectric loss factor decreases with the increase in frequency. This result may be attributed to the fact that with the increase in frequency, the extent of local displacement in the direction of electric field increases that cause an increase in electric polarization, which in turn enhances the dielectric loss.

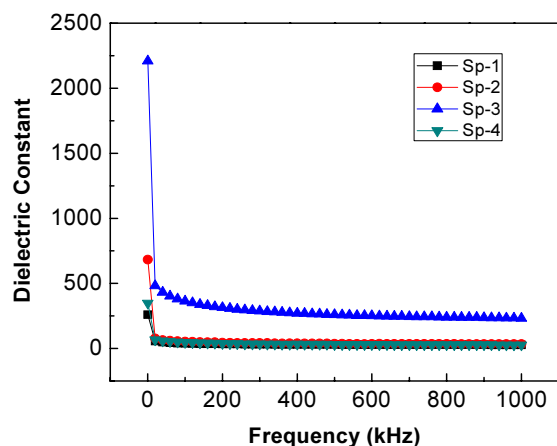


Fig. 3 Comparison of frequency dependent dielectric constants of all the samples

Room temperature measurements of magnetic hysteresis (M-H) loops were performed for all the four samples, as shown in the Fig. 5. The M-H loops of the samples were measured in the powder form. Prior to the magnetization measurements, the powder samples were weighed on a precise digital balance, in order to calculate the magnetization in terms of emu/g. The field was varied in the range of  $\pm 10$  kOe, to obtain the hysteresis curves.

As can be seen in the loops, a ferromagnetic behavior of NiO nanoparticles is evident. The values of magnetization ( $M_s$ ) were found to vary from  $8-14 \pm 1$  emu $g^{-1}$ , as

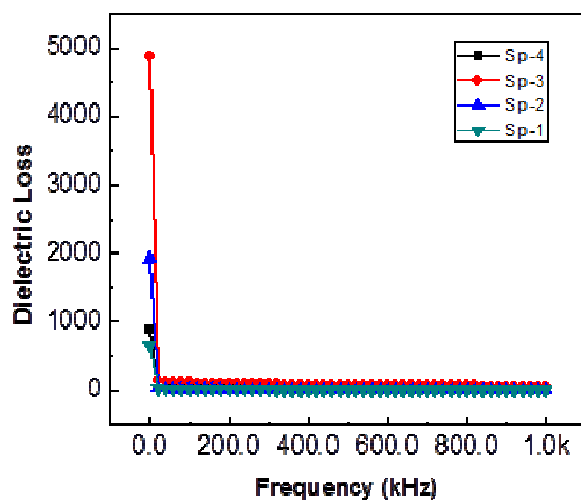


Fig. 4 Comparison of frequency dependent dielectric loss factor of all the samples

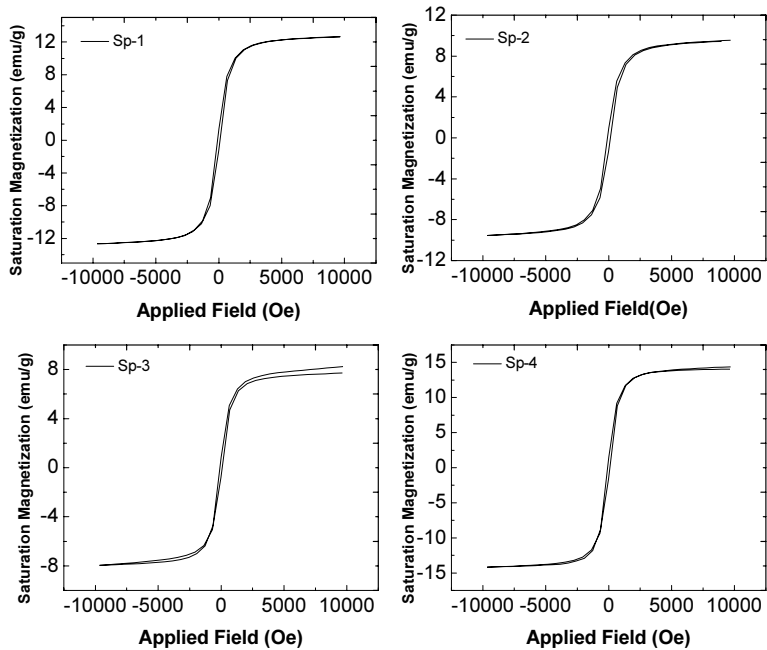


Fig. 5 Magnetic hysteresis loops of samples Sp-1, Sp-2, Sp-3 and Sp-4

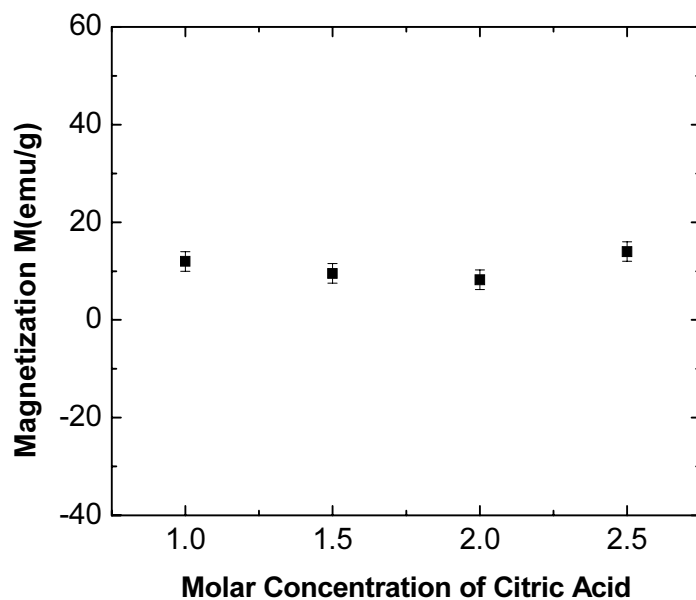


Fig. 6 Effect of molar concentration of citric acid on the magnetization of NiO nanoparticles

shown in Fig. 6. The value of coercive field ( $H_c$ ) was noted to be  $100\pm 5$  Oe in all the samples. This magnetic behavior and the values of magnetization are comparable with the previously reported values by Ichianagi and co-workers (Ichianagi 2007). Traditionally NiO in bulk form exhibits anti-ferromagnetic ordering but it has been shown recently that magnetic ordering in NiO nanoparticles is strongly dependent upon particle size (Peck 2011, Tiwari 2006). In this context, the ferromagnetic behavior shown by our samples could be attributed to the size effect, as the particle size and the crystal structure plays a dominant role in determining the magnetic properties like  $M_s$  and  $H_c$  (Sharma 2007).

#### 4. COMCLUSIONS

Nature and molar concentration of fuel reagents play an essential role in the synthesis of nano-materials, using sol-gel auto-combustion technique. In this study, molar concentration of citric acid is varied, in order to achieve a phase-pure nickel oxide material. The phase-purity was confirmed by X-ray diffraction analysis. The size of the nano-crystallites was  $11.90\pm 0.01$ , as evaluated by the well-known Sherer's formula. The value of dielectric constant decreased with the increase of frequency up to 1 MHz, attributed to the space charge polarization. As far as magnetic properties are concerned, nickel oxide nano-crystallites revealed ferromagnetic behavior exhibiting a magnetization of  $8-14 \text{ emug}^{-1}$ , well justifiable by the previous literature available.

#### Acknowledgements

The first author would like to thank Dr. Saira Riaz and Dr. Muhammad Sabieh Anwar for their help in experimental measurements.

#### REFERENCES

- Aslani, A., Shamili, A.B. and Kaviani, K. (2010), "Sonochemical synthesis, characterization, optical analysis of some metal oxide nanoparticles (MO-NP:M=Ni, Zn and Mn)", *Physica B*, **405**(18), 3972-3976.
- Bahadur, J., Sen, D., Mazumder, S. and Ramanathan, S. (2008), "Effect of heat treatment on pore structure in nano-crystalline NiO: a small angle neutron diffraction study", *J. Solid State Chem.*, **181**(5), 1227-1235.
- Bandara, J. and Yasomanee J.P. (2007), "p-type oxide semiconductors as hole collectors in dye-sensitized solid-state solar cells", *Semicond. Sci. Technol.*, **22**(2), 20-24.
- Ichianagi, Y., Wakabayashi, N., Yamazaki, J., Yamada, S., Kimishima, Y., Komatsu, E. and Tajima, H. (2003), "Magnetic properties of NiO nanoparticles", *Physica B*, **329**(2), 862-863.
- Laishram, R., Phanjobam, S., Sarma, H.N.K. and Prakash, C. (1999), "Electrical and magnetic studies of the spinel system  $L_{1-0.5+t}Cr_xSb_tFe_{2.5-x-2t}O_4$ ", *J. Phys. D: Appl. Phys.*, **32**(17), 2151-2154.
- Levy, B. (1997), "Photochemistry of nanostructured materials for energy applications", *J. Electroceram.*, **1**(3), 239-272.

- Liao, C.L., Lee, Y.H., Chang, S.T. and Fung, K.Z. (2006), "Structural characterization and electrochemical properties of RF-sputtered nanocrystalline  $\text{Co}_3\text{O}_4$  thin-film anode", *J. Power Sources*, **158**(2), 1379-1385.
- Meybodi, S.M., Hosseini, S.A., Rezaee, M., Sadrnezhad, S.K. and Mohammadyani, D. (2012), "Synthesis of wide band gap nanocrystallite NiO powders via a sonochemical method", *Ultrason. Sonochem.*, **19**(4), 841-845.
- Mohammadyani, D., Hosseini, S.A. and Sadrnezhad, S.K. (2009), "Characterization of nickel oxide nanoparticles synthesized via rapid microwave-assisted route", *Proceeding of Second International Conference on Ultrafine Grained and Nanostructured Materials Center of Excellence For High Performance*, Materials School of Metallurgy and Materials Engineering University, College of Engineering, University of Tehran, Tehran, Iran.
- Murray, C.B., Kagan, C.R. and Bawendi, M.G. (2000), "Synthesis and characterization of monodisperse nanocrystals and closed-packed nanocrystal assemblies", *Annu. Rev. Mater. Sci.*, **30**(1), 545-610.
- Peck, M.A., Huh, Y., Skomski, R., Zhang, R., Kharel, P., Allison, M.D., Sellmyer, D.J. and Langell, M.A. (2011), "Magnetic properties of NiO and (Ni, Zn)O nanoclusters", *J. Appl. Phys.*, **109**(7), 07B518-1 - 3.
- Pei, G., Wu, F., Xia, C., Zhang, J., Li, X. and Xu, J. (2008), "Influences of Al doping concentration on structural, electrical and optical properties of  $\text{Zn}_{0.95}\text{Ni}_{0.05}\text{O}$  powders", *Curr. Appl. Phys.*, **8**(1), 18-23.
- Poulston, S., Faraldi, P., Hyde, T.I., Pidria, M.F., Houel, V. and Wagland, A. (2005), "Characterization of protective coatings for planar automotive gas sensors", *Sens. Actuators B*, **110**(2), 209-217.
- Qiao, H., Wei, H. Yang, H. and Yan, X. (2009), "Preparation and characterization of NiO nanoparticles by anodic arc plasma method", *J. Nanomater.*, **1**(1), 1-5.
- Richardson, J.T., Scates, R. and Twigg, M.V. (2003), "X-ray diffraction study of nickel oxide reduction by hydrogen", *Appl. Catalysis A: General*, **246**(1), 137-150.
- Shaikh, A.M., Bellad, S.S. and Chougule, B.K. (1999), "Temperature and frequency-dependent dielectric properties of Zn substituted Li-Mg ferrites", *J. Magn. Magn. Mater.*, **195**(2), 384-390.
- Sharma, V.K., Xalxo, R. and Varma, G.D. (2007), "Structural and magnetic studies of Mn-doped ZnO", *Cryst. Res. Technol.*, **42**(1), 34-38.
- Tiwari, S.D. and Rajeev, K.P. (2006), "Magnetic properties of NiO nanoparticles", *Thin Solid Films*, **505**(1-2), 113-117.
- Ulmane, N.M., Kuzmin, A., Grabis, J., Sildos, I., Voronin, V.I., Berger, I.F. and Kazantsev, V.A. (2011), "Structural and magnetic properties of nickel oxide nanoparticles", *Solid State Phenom.*, **168**(1), 341-344.